Available online at www.sciencedirect.com
SCIENCE DIRECT®
Construction and Building Materials 18 (2004) 767–779
Construction and Building MATERIALS
www.elsevier.com/locate/conbuildmat

Span ratios in bridges constructed using a balanced cantilever method

Hyo-Gyoung Kwak *, Je-Kuk Son

Department of Civil Engineering, Korea Advanced Institute of Science and Technology, 373-1 Kusong-dong, Yusong-gu, Taejon 305-701, Republic of Korea

Received 25 March 2003; received in revised form 6 April 2004; accepted 8 April 2004
Available online 31 July 2004

Abstract

This paper introduces a relation to determine the span ratio between exterior and interior spans, which is required in the preliminary design stage of bridges constructed by balanced cantilever method. On the basis of the numerical results obtained by rigorous time-dependent analyses and by the simple equations introduced in the companion paper, the moment distribution along the spans and its variation with the construction sequence are reviewed, and a recommendation for a rational design is suggested. First, a relation for the initial tendon force is derived on the basis of an assumption that no vertical drift occurs at the far end of a cantilever beam due to the balanced condition between the self-weight and the cantilever tendons. In advance, the determination of an effective span ratio is followed with an assumption that the magnitude of maximum negative moment must be the same as that of the maximum positive moment along all of the spans. Finally, many rigorous time-dependent analyses are conducted to establish the validity of the introduced relations, and this paper shows that an effective span length ratio of the exterior span to the interior span ranges between 0.75 and 0.8.

Keywords: Balanced cantilever method; RC bridges; Construction sequence; Creep; Span length; Relaxation

1. Introduction

Balanced cantilever construction simply cantilevers segments from a pier in a balanced fashion on each side until the midspan is reached and a closure is made with a previous half-span cantilever from the preceding pier. The same erection process is repeated until the structure is completed. As mentioned in the companion paper, balanced cantilever segmental construction has long been recognized as one of the most efficient methods of building bridges as it does not require falsework. This method has great advantages over other forms of construction in urban areas where temporary shoring would disrupt traffic and services below, and over waterways where falsework would not only be expensive but also a hazard.

Cantilever construction was first introduced in Europe in the early 1950s, and it has since been broadly used in the design and construction of several hundred bridges. Unlike several large bridges built in Germany using cast-in-place segments, cantilever construction in France took a different direction, emphasizing the use of precast segments. Comparing cast-in-place segmental construction with precast segmental construction, the following features come to mind: cast-in-place segmental construction is a relatively slow construction method. The work is performed in situ, i.e., exposed to weather conditions. The time-dependent deformations of concrete become very important as a result of early loading of the young concrete [8–11]. On the other hand, precast segmental construction is a relatively fast construction method determined by the time required for the erection. The major part of the work is performed in the precasting yard, where it can be

* Corresponding author. Tel.: +82-42-869-3621; fax: +82-42-869-3610.
E-mail address: khg@kaist.ac.kr (H.-G. Kwak).

0950-0618/$ - see front matter © 2004 Elsevier Ltd. All rights reserved.
doi:10.1016/j.conbuildmat.2004.04.022

protected against inclement weather. Precasting can start simultaneously with the foundation work. The time-dependent deformations of the concrete become less important, as the concrete may have reached a higher age by the time the segments are placed in the structure. From 1960s, the construction method has undergone refinements, and many variations of the basic concept have been developed to adopt the method to specific conditions of a project and to achieve more effective bridge construction [1,2].

In parallel with the improvement in construction method, many efforts to reach to an optimum design have been undertaken [3,15]. In the transverse direction, classical optimization approaches on the basis of mathematical programming methods, which have an object function of the total weight and constraint equations of stress and deflection limits, have been performed [12,14], and limit dimensions for each part in a cross section have been introduced even though the dimensions of each part largely depend on structural considerations as well as on practical factors related to the production and handling of the segments.

In selecting the span arrangement for a segmental bridge constructed by the balanced cantilever method, it is also necessary to consider the construction sequence along the span length in the longitudinal direction. If the end span is selected as 65–70% of the interior span, only a small portion of the superstructure adjacent to the abutment will require use of falsework or some other erection procedure different from balanced cantilever construction. However, to determine an optimum span length ratio between the end span and the interior span, more rigorous numerical analyses that consider the construction sequence and the time-dependent behavior of the structure must be conducted [4,6–8,11].

When laying out spans for bridges, an equal span system is often used in medium to short-span bridges because it provides a maximum standardization of elements. However, the application of unequal span construction is also possible and in certain cases more favorable. Many parametric studies for the span length ratio and the depth-length ratio have been conducted to reach to an optimum design for a few bridge types [3,15]. Within long-span bridges, in particular, the end span length must be shorter than that of the interior spans. Since relatively larger bending moments are generally occur at the end span in a multi-span continuous bridge because of the boundary condition, the end span length needs to be reduced to decrease the positive and negative bending moments at the end span, which are proportional to a square of the span length, so that the moment difference between the end span and the adjacent interior span decreases and more rational design can be induced. Specifically, the determination of an effective span length ratio between the end span and the interior span may be one approach that could result in an optimum design.

Taking these characteristic into account, a relation to determine an effective span length ratio in a bridge constructed by the balanced cantilever method is introduced in this paper, on the basis of the deflection condition at the end of the cantilevered span during construction and the moment equality at the end span and the adjacent interior span. Several numerical examples are given to investigate the validity of the introduced relation, and a recommendation for the determination of an effective span length ratio for a rational design is also suggested.

2. Moment variation during construction

To verify the effectiveness of the relations introduced in the companion paper, the internal moment variations by the dead load and cantilever tendons calculated for FCM 1, FCM 2, and FCM 3 bridges (see Fig. 1 in the companion paper), which were obtained through rigorous time-dependent analyses that considered the construction sequence [4,6–8,11], are compared with those obtained by the superposition of Eqs. (5) and (6) introduced in the companion paper. All the material properties used in the numerical analyses are the same with those mentioned in Tables 1 and 2 in the companion paper. Figs. 1–3, representing the obtained results at $t = 1$ year, $t = 10$ years, and $t = 100$ years after completion of construction for each bridge, show that the superposition of two relations representing the dead load moment (Eq. (5) in the companion paper) and the cantilever tendon moment (Eq. (6) in the companion paper) effectively simulates the internal moment variation with time regardless of the construction sequence.

In advance, as in the dead load moment alone, the superposition of two equations for the dead load and cantilever tendon moments also gives slightly larger positive moments than those obtained by rigorous analysis along the spans (see Figs. 1–3). On the other hand, the exactness for the negative moment values at the internal supports, where the maximum negative moments occur, depends on the accuracy of the relation for the cantilever tendon moment as well as that for the dead load moment. Since Eqs. (5) and (6) in the companion paper effectively simulate the dead load and cantilever tendon moments along the span, respectively, the moment distribution by the superposition of both two equations also gives the negative moment distributions which represent less differences than those caused in the case of the dead load moment alone. Nevertheless, the maximum negative de-

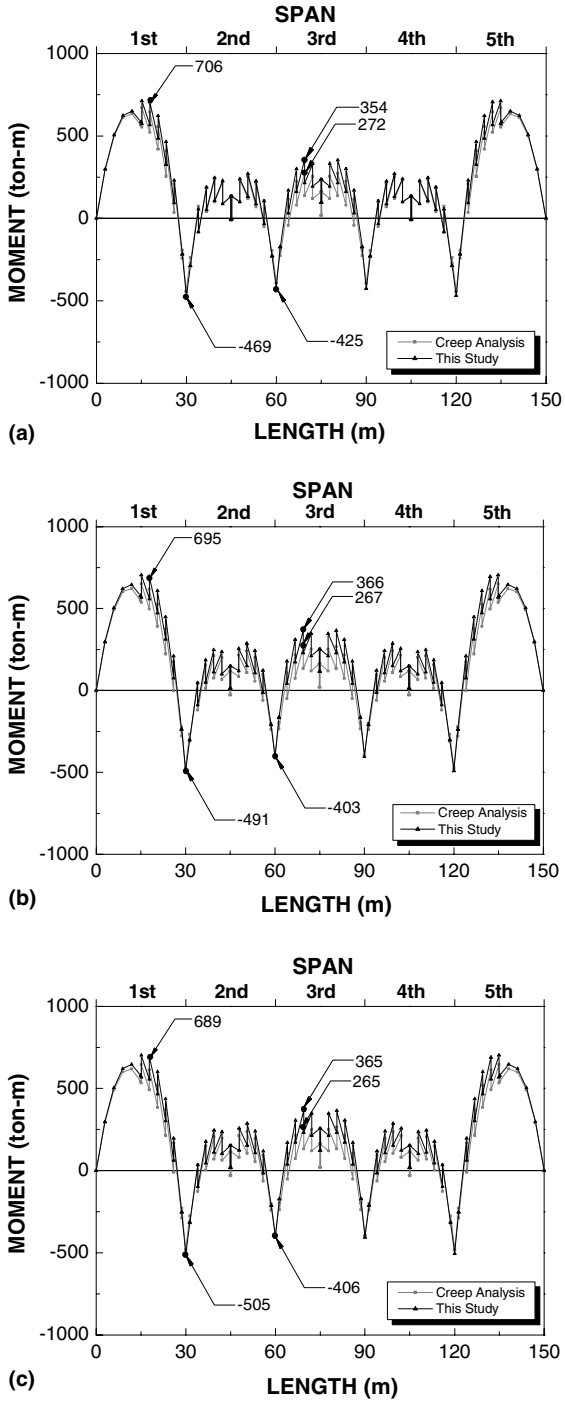

Fig. 1. Moment variations of FCM 1 bridge: (a) after 1 year; (b) after 10 years; (c) after 100 years.

sign moment which must be taken in the preliminary design stage can be determined as a constant value of

$$M = M_{\mathrm{D}} + M_{\mathrm{T}} = w_{\mathrm{D}} \cdot l^2/8 + P_i \cdot e \cdot n \cdot \chi$$
$$= -1160t \cdot m + 117t \times 1.3m \times 5^{\mathrm{EA}} \times 0.82$$
$$= -536.4t \cdot m,$$

where n is the number of cantilever tendons and χ is the aging coefficient of concrete, on the basis of the cantilevered state because this maximum value gradually decreases with an increase of the positive moment at the midspan according to the continuity of each span.

Figs. 1–3 show that the maximum positive and negative moments generally occur at the end spans due to the boundary conditions at both ends, which represent no rigidity for the moment resistance. Accordingly, to move towards a more rational design, a reduction of positive and negative moments at the end spans, which represent the largest values, and an increase of positive moments at the internal spans, which show relatively small values, need to be sought. On these aspects, this paper introduces a relation to determine the span ratio between exterior and interior spans, by which the moment differences can be minimized and more rational section dimensions can be determined along the spans.

3. A Proposed design recommendation

3.1. Determination of cantilever tendon force

The cantilevers in FCM bridges are usually constructed by sequential connection of 3–6 m long segments with cantilever tendons. If each cantilever is composed of m-segments of the length l_1 as shown in Fig. 4, the total length of cantilever beam L_1 can be calculated by $L_1 = (n + 0.5) \cdot l_1$. Because of the characteristic in the construction sequence, the downward deflection δ_A by the dead load w and the upward deflection δ_B by the cantilever tendon force P occur at the end of the cantilever (see Fig. 5(a) and (b)). In advance, the deck portion of the end spans adjoining the abutment cannot be erected in a balanced cantilever but is generally completed by the full staging method. This requires that the vertical deflections δ_A and δ_B be the same so that the end spans can be closed without application of any additional force to integrate two parts.

Fig. 4 shows that the first cantilever tendon is installed after concreting the second segment ②, and this causes the cantilever tendon moment calculated by $P \cdot e$ to the segments ① and ② connected previously. The same erection procedure is repeated until midspan is reached. Fig. 5(c) represents the moment distributions by the cantilever tendons representing the terraced distribution ((B) in Fig. 5(c)) and by the uniformly distributed dead load ((A) in Fig. 5(c)). On the basis of the compatibility condition of $\delta_A = \delta_B$, each deflection component may be calculated by the conjugate beam method and can be expressed as:

$$\delta_A = \frac{wL_1^4}{8} \cdot \frac{1}{EI}, \tag{1}$$

Table 1
Comparison of bending moments in both Approaches I

Moments		$(2L_1+0.3)m=30m$	$(2L_1+0.3)m=60m$
Proposed equation (ton/m)	$M_{\text{ext.}}^{+\max}$ (7)	427.5	1494.3
	$M^{-\max}$ (8)	−427.3	−1494.5
	$M_{\text{int.}}^{-\max}$(9)	275.3	884.5
	$\lvert M^{-\max}/M_{\text{ext.}}^{+\max}\rvert$	1.00	1.00
Rigorous analysis (ton/m)	$M_{\text{ext.}}^{+\max}$	407	1399
	$M^{-\max}$	−538	−1939
	$M_{\text{int.}}^{+\max}$	249	770
	$\lvert M^{-\max}/M_{\text{ext.}}^{+\max}\rvert$	1.32	1.39

Table 2
Comparison of bending moments in both Approaches II

Moments		$(2L_1+0.3)m=30m$	$(2L_1+0.3)m=60m$
Proposed equation (ton/m)	$M_{\text{ext.}}^{+\max}$ (7)	427.5	1494.3
	$M_{\text{int.}}^{-\max}$ (8)	−427.3	−1494.5
	$M_{\text{int.}}^{-\max}$(9)	275.3	884.5
	$\lvert M^{-\max}/M_{\text{ext.}}^{+\max}\rvert$	1.00	1.00
Rigorous analysis (ton/m)	$M_{\text{ext.}}^{+\max}$	456	1581
	$M^{-\max}$	−458	−1595
	$M_{\text{int.}}^{+\max}$	320	998
	$\lvert M^{-\max}/M_{\text{ext.}}^{+\max}\rvert$	1.00	1.01

$$\delta_B = \frac{1}{EI}\left[\frac{PeL_1^2}{2} + Pe\cdot\left(L_1 - \frac{L_1}{n+0.5}\right)\cdot\left(\frac{L_1}{n+0.5}\cdot + \frac{1}{2}\left(L_1 - \frac{L_1}{n+0.5}\right)\right) + Pe\cdot\left(L_1 - 2\cdot\frac{L_1}{n+0.5}\right)\cdot\left(2\cdot\frac{L_1}{n+0.5} + \frac{1}{2}\left(L_1 - 2\cdot\frac{L_1}{n+0.5}\right)\right) + \cdots + Pe\cdot\left(L_1 - (n-1)\cdot\frac{L_1}{n+0.5}\right)\cdot\left((n-1)\cdot\frac{L_1}{n+0.5} + \frac{1}{2}\left(L_1 - (n-1)\cdot\frac{L_1}{n+0.5}\right)\right)\right] = \frac{PeL_1^2}{2EI}\cdot\sum_{i=1}^{n}\left(1 - \frac{(i-1)}{n+0.5}\right)\left(1 + \frac{(i-1)}{n+0.5}\right). \quad (2)$$

From the equality of these two relations, the cantilever tendon force P can be finally expressed by

$$P = \frac{wL_1^2}{4e\cdot\sum_{i=1}^{n}\left(1 - \frac{(i-1)}{n+0.5}\right)\left(1 + \frac{(i-1)}{n+0.5}\right)}, \quad (3)$$

where e is the eccentricity of the cantilever tendon with respect to the centroid of a section, n is the number of cantilever tendons arranged, and w is the uniformly distributed dead load.

3.2. Determination of effective span length ratio

The span arrangement for a bridge depends on the method of construction. When cantilever construction is used, the segments are erected in balanced cantilever starting from a pier and placing segments on either side in a symmetrical operation. This method of erection results in typical superstructure components consisting of one-half of the main span length cantilevered from the piers as shown in Fig. 4. In advance, since the end span length must be selected as more than fifty percent of the interior span length to remove the uplift of the superstructure at the end support, regardless of the method of construction, the portion exceeding 50% of the superstructure adjacent to the abutment will require use of falsework or some other erection procedure.

In spite of a relatively short span length, the end span represents the maximum positive and negative moments because of the simply-supported boundary condition at both far ends (see Figs. 1–3). Therefore, for the design to become more rational, a decrease of these maximum moments with an increase of relatively small moments occurred at the interior spans must be achieved so that a multi-span continuous bridge represents the uniformly distributed moment variation along the entire spans. That is to say, more attention must be given to the moment variation at the end spans. Since the section design is conducted on the basis of the maximum mo-

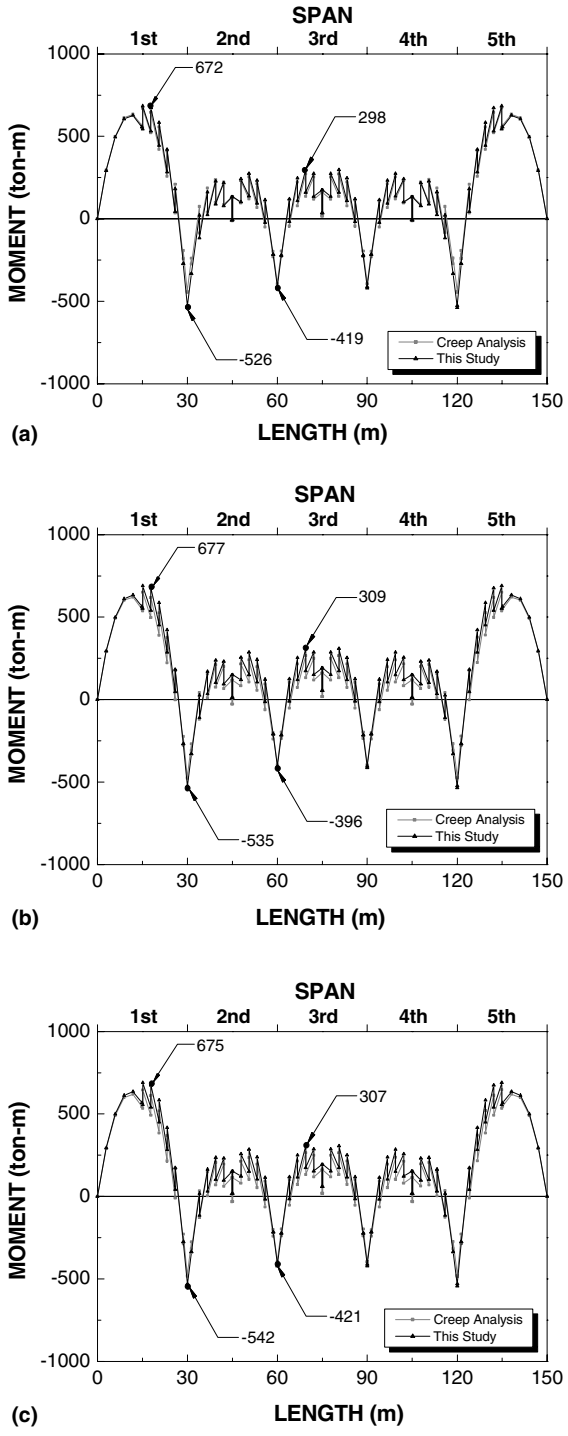

Fig. 2. Moment variations of FCM 2 bridge: (a) after 1 year; (b) after 10 years; (c) after 100 years.

ment envelope, fewer differences moment variations between the internal spans and in the end spans mean that no exceptional considerations for the end spans are required in the design procedure and the same bridge sections can be used along the entire spans regardless of the span location and arrangement. On these backgrounds, this paper introduces a simple relation for an effective span length ratio that derives the uniform moment variation along the entire span.

As shown in Figs. 1–3 in this paper and in Figs. 2–4 in the companion paper, the difference in construction steps does not have a great influence on the final moment distributions, but there is remarkable difference in the final moments between the initially completed continuous bridge (TS in Figs. 1–3) and the balanced

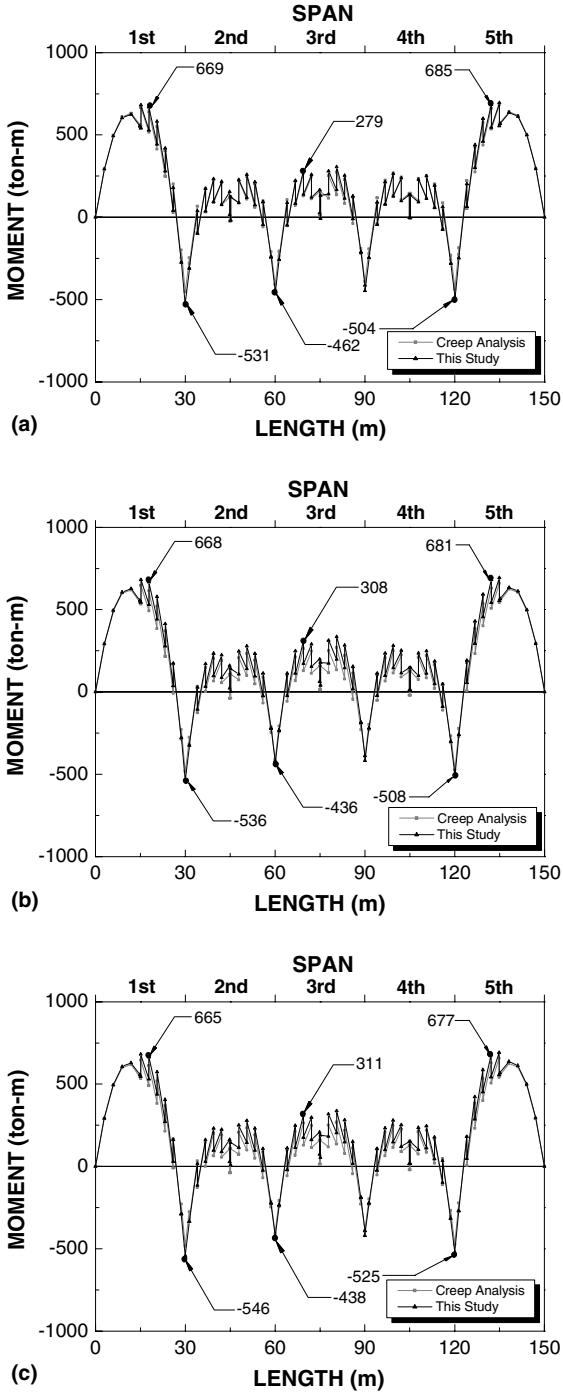

Fig. 3. Moment variations of FCM 3 bridge: (a) after 1 year; (b) after 10 years; (c) after 100 years.

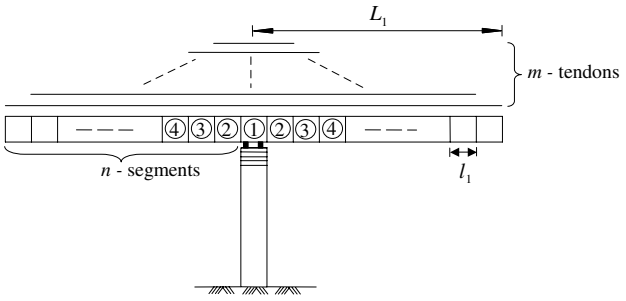

Fig. 4. A cantilevered beam.

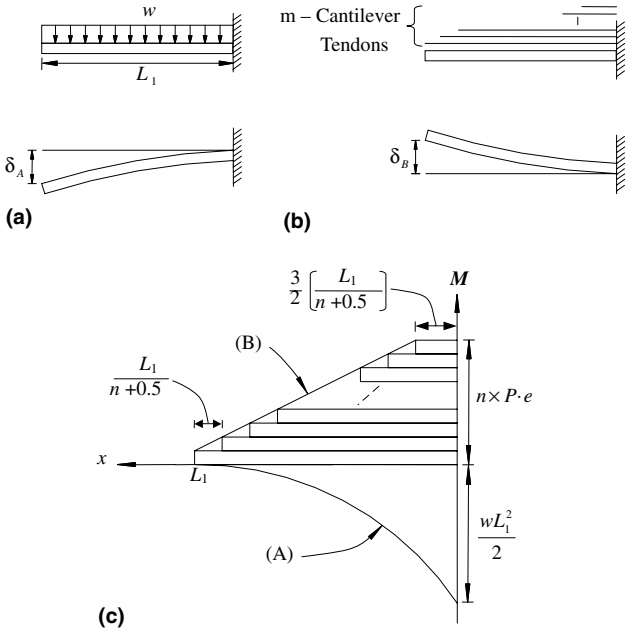

Fig. 5. Structural behavior of a cantilevered beam: (a) downward deflection by dead load; (b) upward deflection by cantilever tendons; (c) moment variation along the cantilever.

cantilever bridges. On the other hand, the moments in the balanced cantilever bridges after completion of the construction ($t = 100$ days) represent an immaterial variation because the relatively large creep deformation of concrete at early ages, up to $t = 100$ days does not contribute to the moment variation.

Therefore, the maximum moments experienced during construction can be calculated on the basis of a statically determinate structure that gives the maximum positive or negative moment. That is, the statically determinate structure shown in Fig. 6 can be taken as a reference structural system because this system gives the largest maximum positive and negative moments through all of the construction steps, and the corresponding maximum values represent minor variations due to creep deformation of concrete even after change in the structural system with a closure of the adjacent interior midspan.

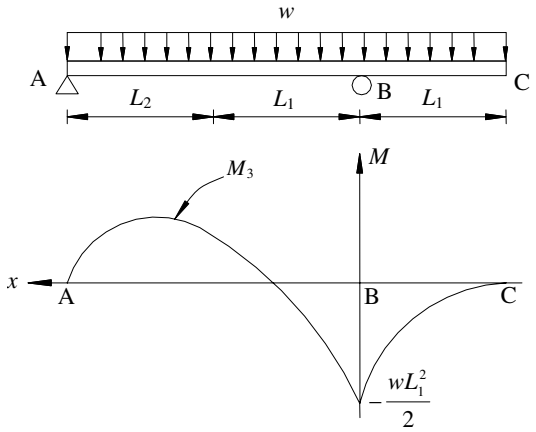

Fig. 6. Description of reference structural system.

Since the interior span in the reference structural system described in Fig. 6 still remains in an overhanged state, as shown in Fig. 5, the negative moment by the dead load M_1^- and the positive moment by the cantilever tendons M_2^+ at the interior span (the region bounded by two points of B and C in Fig. 6) can be expressed by:

$$M_1^- = -\frac{1}{2}w(L-x)^2, \tag{4}$$

$$M_2^+ = Pen \quad \text{when } 0 \leqslant x \leqslant \frac{3}{2}\frac{L_1}{(n+0.5)}$$

$$= Pen - Pe\frac{(n+0.5)}{L_1}\left(x - \frac{3}{2}\frac{L_1}{(n+0.5)}\right)$$

$$\text{when } \frac{3}{2}\frac{L_1}{(n+0.5)} \leqslant x \leqslant L_1, \tag{5}$$

where x is the distance from the interior support point B in Fig. 6.

On the other hand, the positive and negative moments by the dead load at the exterior span of the reference structural system represents the values of $M_{\max}^- = 1159t - m$ and $M_{\max}^+ = 652t - m$ when $L_1 = L_2 = 15$ m in Fig. 6. The same section properties mentioned in Tables 1 and 2 in the companion paper are used. The moment distribution obtained is shown in Fig. 7. From the comparison of the results in Fig. 7 with those in Figs. 2–4 in the companion paper, the following can be inferred: (1) the moments represent almost the same values in spite of having different structural systems, indicating that the moment variation induced by the change in the structural system with a connection of the adjacent interior span is negligibly small; and (2) the moment distribution by the dead load at the exterior span can be simulated on the basis of the reference structural system in Fig. 6, regardless of the structural system and time considered. Based on these aspects, the moment distribution at the exterior span can be expressed by

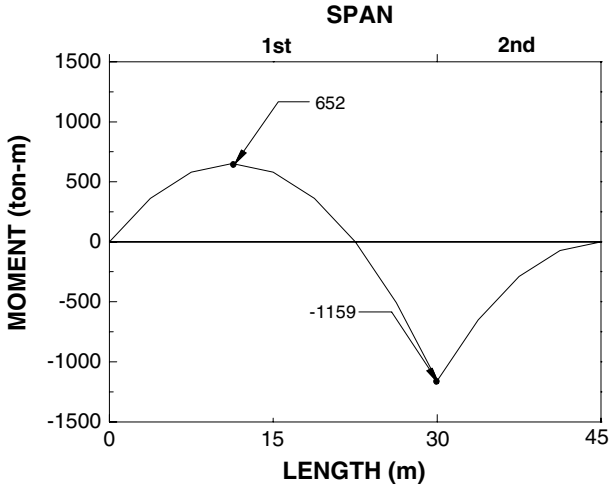

Fig. 7. Moment distribution of reference structural system.

$$M_3 = \frac{w(2L_1 + L_2)^2}{2(L_1 + L_2)} \cdot x - \frac{w}{2}(L_1 + x)^2, \tag{6}$$

where x is the distance from the interior support point B in Fig. 6.

On the basis of the moment distributions, the moment at the exterior span can be represented by the superposition of two moment components of M_2^+ by the cantilever tendons (see Eq. (5)) and M_3 by the dead load in the reference structural system (see Eq. (6)). Similarly, the moment at the interior span can also be expressed by the superposition of two moment components of M_1^- by the dead load (see Eq. (4)) and M_2^+ by the cantilever tendon (see Eq. (5)), and the end moment at point B can be determined as

$$M^{-\max} = -\frac{1}{2}wL_1^2 + Pen. \tag{7}$$

In other words, the positive moments at the exterior span and at the adjacent interior span can be expressed by Eqs. (8) and (9), respectively. In advance, their maximum values are determined from the first derivation of the moment with respect to $x(\mathrm{d}M/\mathrm{d}x = 0)$ within the interval of $1.5L_1/(n+0.5) \leqslant x \leqslant L_1$, and x values determined are $x = (2L_1 + L_2)^2/(2L_1 + 2L_2) - Pe(n+0.5)/(wL_1) - L_1$ for $M_{\text{ext.}}^+$, and $x = L_1 - Pe(n+0.5)/(wL_1)$ for $M_{\text{int.}}^+$.

$$\begin{aligned} M_{\text{ext.}}^+ &= M_2 + M_3 \\ &= Pen - Pe\frac{(n+0.5)}{L_1}\left(x - \frac{3}{2}\frac{L_1}{(n+0.5)}\right) \\ &\quad + \frac{w(2L_1 + L_2)^2}{2(L_1 + L_2)} \cdot x - \frac{w}{2}(L_1 + x)^2, \end{aligned} \tag{8}$$

$$\begin{aligned} M_{\text{int.}}^+ &= M_1 + M_2 \\ &= -\frac{1}{2}w(L_1 - x)^2 + Pen \\ &\quad - Pe\frac{n+0.5}{L_1}\left(x - \frac{3}{2}\frac{L_1}{(n+0.5)}\right). \end{aligned} \tag{9}$$

As shown in Eqs. (7)–(9), the maximum positive moment at the interior span $M_{\text{int.}}^{+\max}$ and the negative moment at the first interior support $M^{+\max}$ can be determined using the tendon force P in Eq. (3), the eccentricity e, and the interior span length $(2L_1 + 0.3m)$. The positive moment at the exterior span is a function of its span length expressed by $L_1 + L_2$, so that the magnitude of the maximum positive moment at the exterior span depends on the length L_2 as well as the length L_1. Therefore, to determine the reference positive moment for the comparison with the negative moment at the interior support, the relative magnitudes of both positive moments need to be reviewed. Eq. (10) representing this difference always has a positive value regardless of changes in design variables because the first term $(C-2)$ and the second term $(0.5wL_1^2C - BL_1)$ have positive values except $L_2 = 0$ at which $C = 2$.

$$M_{\text{ext.}}^{+\max} - M_{\text{int.}}^{+\max} = (C-2)(0.5wL_1^2C - BL_1), \tag{10}$$

where

$$\begin{aligned} &0.5wL_1^2C - BL_1 \\ &= 0.5wL_1^2C - (0.5+n)Pe = wL_1^2\left[0.5C - (0.5+n)\right. \\ &\quad \left.\Big/\left(4\sum_{i=1}^{n}\left(1 - \frac{(i-1)}{n+0.5}\right)\left(1 + \frac{(i-1)}{n+0.5}\right)\right)\right] > 0, \end{aligned} \tag{11}$$

$C = (2+k)^2/(2+2k)$, $B = (n+0.5)Pe/L_1$, $L_2 = kL_1$, and k the proportional constant. Since L_2 must be greater than zero, the maximum positive moment will occur at the exterior span in the balanced cantilever bridge. That is to say, the magnitude of the positive moment is always governed by that of the exterior span.

As mentioned before, the bridges constructed by the balanced cantilever method represent the internal moment redistribution which takes place over the service life of a structure because of the time-dependent deformations of concrete and changes in the structural system repeated during construction. That is, an increase of the positive moment as well as a decrease of the negative moment is accompanied with time, but the absolute difference between the negative moment and the positive moment maintains a constant value at a span due to the force equilibrium equation. Therefore, a rational and economical design of the balanced cantilever bridge may be initiated through the minimization of the moment difference between the negative moment at the interior

support and the positive moment at the exterior span. In this case, the same section can be used along the entire span, and a greater concentration of internal moment can be released to the exterior span.

On these aspects, the exterior span length $L_1 + L_2$ can be inferred from the condition of $M_{\text{ext.}}^{+\max} + M^{-\max} = 0$, and it gives the following relation:

$$A_1 \cdot A^2 + B_1 \cdot A + C_1 = 0, \tag{12}$$

$$A = \frac{-B_1 \pm \sqrt{B_1^2 - 4A_1C_1}}{2A_1} \left(B_1^2 - 4A_1C_1 \geqslant 0\right), \tag{13}$$

where $A = (2L_1 + L_2)^2/(2L_1 + 2L_2) = (2 + k)^2 L_1/(2 + 2k) = CL_1$, $A_1 = w/2$, $B_1 = -B - L_1 w$, and $C_1 = 1.5Pe + BL_1 + 2nPe + B/(2w) - wL_1^2/2$.

Since an expression of $A = (2L_1 + L_2)^2/(2L_1 + 2L_2)$ can be rearranged with respect to the length L_2 as Eq. (14), the exterior span length calculated by $L_1 + L_2$, which leads to a rational design, can finally be determined.

$$L_2^2 + (4L_1 - 2A)L_2 + 4L_1^2 - 2AL_1 = 0, \tag{14}$$

$$L_2 = -(2L_1 - A) \pm \sqrt{(2L_1 - A)^2 - (4L_1^2 - 2AL_1)}, \tag{15}$$

where $(2L_1 - A)^2 - (4L_1^2 - 2AL_1) \geqslant 0$.

4. Applications

Using Eqs. (3) and (15), the tendon force of the cantilever tendons and the exterior span length in a balanced cantilever bridge can be determined. Fig. 8 shows the span length ratio SLR ($\text{SLR} = (L_1 + L_2)/(2L_1 + 0.3)$, where $0.3m$ is the length of a key segment at midspan) obtained by the rigorous time-dependent analyses considering the construction sequence and arranged with respect to the cantilevered beam length L_1. As shown in this figure, the exterior span length $(L_1 + L_2)$ must be $0.75 \sim 0.77$ times the interior span length $(2L_1 + 0.3m)$ to be a rational and economical design regardless of the interior span length. The optimum span length ratio represents the maximum value of 0.77 when the internal span length reaches to $(2L_1 + 0.3)m = 50.3m$ and converges to a value of 0.755 as the interior span length gradually increases.

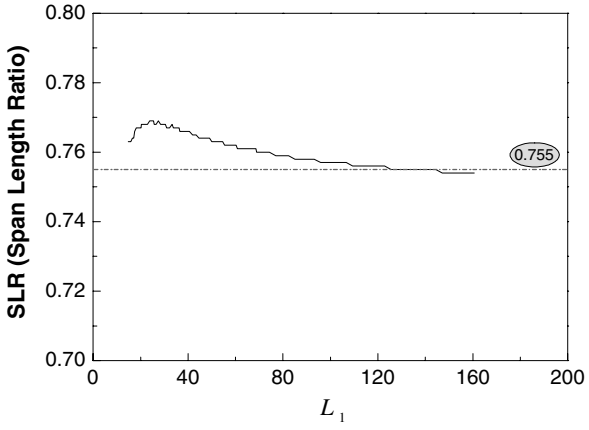

Fig. 8. Relation between SLR and L_1.

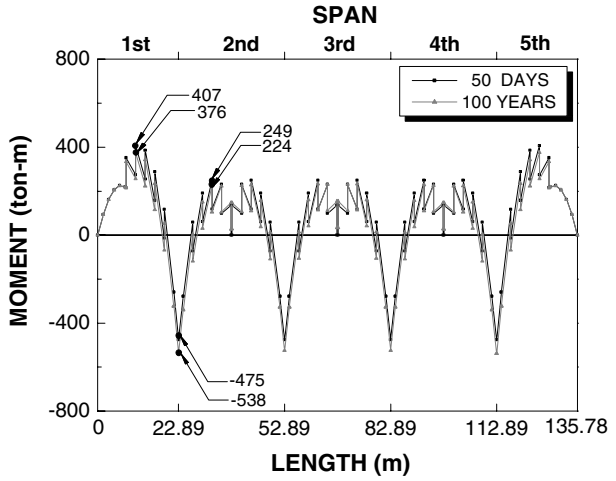

Fig. 9. Moment distribution in FCM 2 bridge with SLR = 0.763, $(2L_1 + 0.3)m = 30m$, and $P = 108975.9$ kg.

In advance, Figs. 9 and 10 represent the moment distribution by the dead load and the cantilever tendon force determined from a rigorous time-dependent analysis, when the internal span lengths $(2L_1 + 0.3m)$ are $30m$ and $60m$, respectively. FCM 2 in the companion paper is assumed, and the time-dependent rigorous analyses are conducted on the basis of the length $L_2 = 8.04m$ and $L_2 = 16.23m$ from Eq. (15) and $P = 108975.9$ and $P = 238020.0$ kg from Eq. (3), respectively. The cantilever tendon area A_P is assumed by $P/0.8f_{py}$ and the

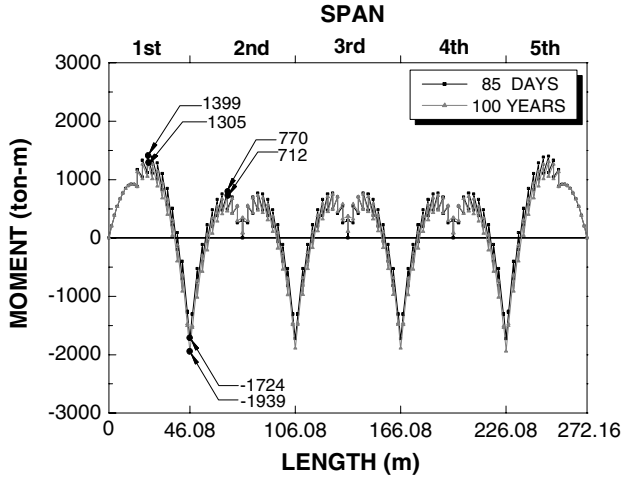

Fig. 10. Moment distribution in FCM 2 bridge with SLR = 0.768, $(2L_1 + 0.3)m = 60m$, and $P = 238020.0$ kg.

corresponding number of segments are assumed to be $n = 5$ and $n = 10$, respectively.

Table 1 also shows the comparison of the bending moments obtained in Figs. 9 and 10 with those calculated by the proposed equations of (7)–(9) in this paper. As shown in this table, the proposed equations give an unit value for the absolute moment ratio at the exterior span $|M^{-\max}/M^{+\max}_{\text{ext.}}| = 1.0$, regardless of the internal span length, while these ratios, determined on the basis of the numerical results obtained by the rigorous analysis, represent slightly different values from $|M^{-\max}/M^{+\max}_{\text{ext.}}| = 1.0$. These differences seem to be caused by the relaxation of cantilever tendons. Unlike the introduced equations in which the relaxation effect is excluded in the derivation procedure, here the relaxation effect is taken into account in the rigorous time-dependent analysis according to the ACI model. In the case of balanced cantilever bridges, the dead load moment variation induced by the creep deformation of concrete seems to be small, but the cantilever tendon moment variation induced by the relaxation of tendon force is expected to be relatively large. Therefore, this relaxation effect in the cantilever tendons must be considered.

The use of an initial prestressing force instead of an effective prestressing force, which is revised and estimated by considering the relaxation of tendon force, gives similar results in both the rigorous time-dependent analysis and the introduced simplified equations.

Relaxation of tendon force with time is taken into consideration based on the following equation by Magura et al. [13].

$$R = \frac{f_s}{f_{si}} = 1 - \frac{\log t}{10}\left(\frac{f_{si}}{f_{py}} - 0.55\right) = 1 - \frac{\log t}{40}, \frac{f_{si}}{f_{py}} \geqslant 0.55, \quad (16)$$

where f_s is the stress at time t; f_{si} is the initial stress immediately after stressing; f_{py} is the 0.1% offset yield stress; and t is the time in hours after stressing. Since f_{si} is assumed as $f_{si} = 0.8f_{py}$ in this paper, the stress ratio R can be simplified by $R = 1 - \log t/40$.

Eq. (16) is valid only for the condition in which the strain is kept constant and f_{si} is the only applied stress. Therefore, the total stress relaxation (f_{rn}) at time t_n is obtained by summing up all the relaxation (Δf_{rk}) at each time interval ($t_k - t_{k-1}$), that is $f_{rn} = \sum_{k=1}^{n} \Delta f_{rk}$, according the procedure suggested by Hernandez and Gamble [5].

If $t = 100$ years is assumed, then the stress ratio R has the value of 0.85, and the modified tendon forces considering the relaxation ($P_R = P/R$), equivalent to the initial force, represent $P_R = 128206.9$ and 280023.5 kg in bridges with the internal span lengths of $l = 2L_1 + 0.3m = 30m$ and $l = 60m$, respectively (see Eqs. (3) and (15)). The corresponding tendon areas are also revised in accordance with the changes in the tendon forces and have the values of 10.9 and 23.7 cm^2 from $A_p = P_R/0.8f_{py}$. Numerical results by the rigorous time-dependent analysis using the revised tendon forces and areas are shown in Figs. 11 and 12.

Differently from Figs. 9 and 10, these figures show the moment distributions that almost the same maximum and minimum moments at the exterior span. Table 2 also shows that the moment ratios at the exterior span represent $|M^{-\max}/M^{+\max}_{\text{ext.}}| \cong 1.0$ regardless of the differences in the internal span length and analysis methods even though the moment values differ from each other. Moreover, consideration of the relaxation in the cantilever tendons gives improved moment ratios.

As mentioned before, to be a rational and economical design, the span length ratios of SLR $= (L_1 + L_2)/(2L_1 + 0.3m)$, must be 0.763 and 0.768 when the interior

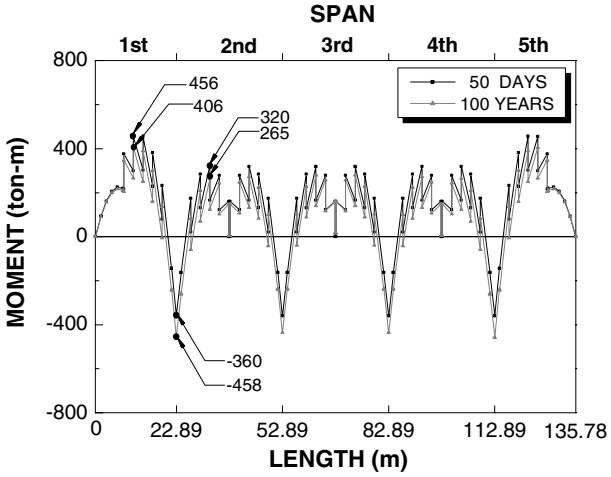

Fig. 11. Moment distribution in FCM 2 bridge with SLR = 0.763, $(2L_1 + 0.3)m = 30m$, and $P_R = 128206.9$ kg.

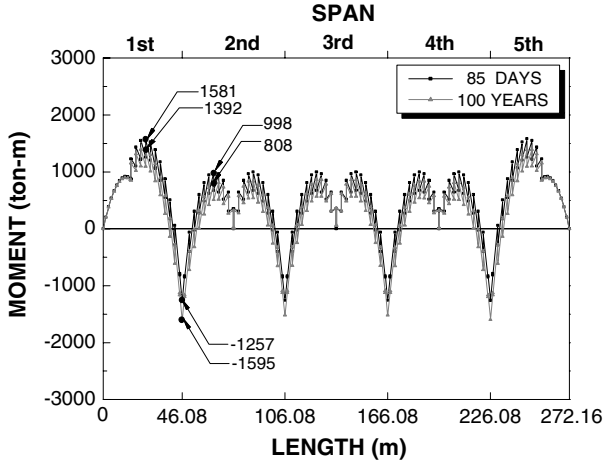

Fig. 12. Moment distribution in FCM 2 bridge with SLR = 0.768, $(2L_1 + 0.3)m = 60m$, and $P_R = 280023.5$ kg.

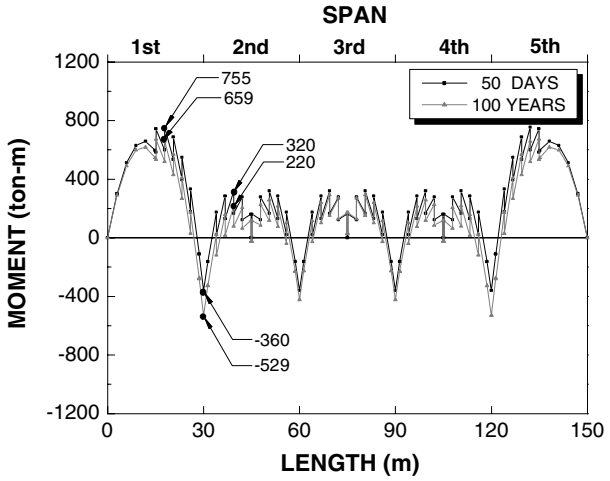

Fig. 13. Moment distribution in FCM 2 bridge with SLR = 1.0, $(2L_1 + 0.3)m = 30m$, and $P_R = 128206.9$ kg.

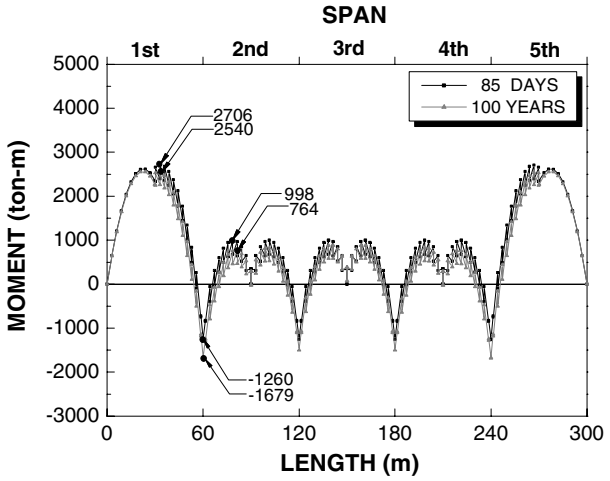

Fig. 15. Moment distribution in FCM 2 bridge with SLR = 1.0, $(2L_1 + 0.3)m = 60m$, and $P_R = 280023.5$ kg.

span lengths are $30m$ and $60m$, respectively. Accordingly, additional parametric studies for different SLR from the optimum values determined on the basis of Eq. (15) are conducted, and typical numerical results for SLR = 1.0 and 0.6 are shown in Figs. 13–16 and also described in Table 3. From these figures and the table, the following can be inferred: (1) as SLR values become further from the optimum values corresponding to each internal span length, differences between the maximum positive and negative moments at the exterior span gradually increase, and this unequal moment distribution may lead to an irrational and uneconomical design; (2) the correction of SLR using Eq. (15) with the use of revised tendon force P_R considering the relaxation must be achieved; and (3) determination of the maximum moments by Eqs. (7)–(9) finally gives the optimum SLR values and gives similar magnitudes for the maximum

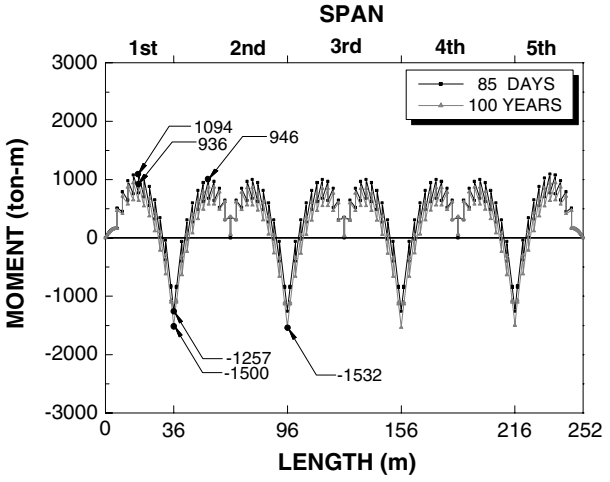

Fig. 16. Moment distribution in FCM 2 bridge with SLR = 0.6, $(2L_1 + 0.3)m = 60m$, and $P_R = 280023.5$ kg.

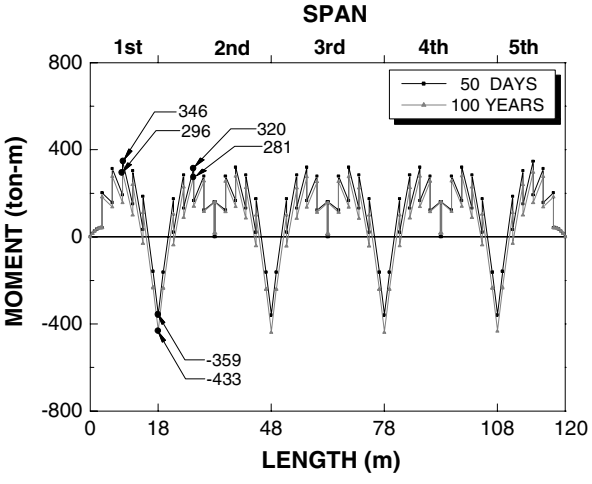

Fig. 14. Moment distribution in FCM 2 bridge with SLR = 0.6, $(2L_1 + 0.3)m = 30m$, and $P_R = 128206.9$ kg.

positive and negative moments at the exterior span, leading to a more rational and economical design.

More parametric studies have been conducted for FCM 2 bridges with different internal span lengths. Figs. 17 and 18 show the relation between the moment ratio at the exterior span $|M^{-\max}/M^{+\max}_{\text{ext.}}|$ and the span length ratio SLR. In Fig. 17, the moment ratios are determined on the basis of a rigorous time-dependent analysis, and the revised tendon force P_R is used so that the relaxation in the cantilever tendons is taken into consideration with time. On the other hand, the moment ratios in Fig. 18 are analytically calculated on the basis of the introduced simple Eqs. (7)–(9) with the effective tendon force.

As shown in these figures, the moment ratios to the span length ratio represent similar slopes in both approaches and give the optimum SLR values that show very few differences in spite of wide differences in the

Table 3
Rigorous analysis results with respect to the span length ratios

Moments (ton/m)		SLR = 1	SLR = 0.6
$(2L_1 + 0.3)m = 30m$	$M_{\text{ext.}}^{+\max}$	755	346
	$M^{-\max}$	−529	−433
	$M_{\text{int.}}^{+\max}$	320	320
	$\lvert M^{-\max}/M_{\text{ext.}}^{+\max}\rvert$	0.70	1.25
$(2L_1 + 0.3)m = 60m$	$M_{\text{ext.}}^{+\max}$	2706	1094
	$M^{-\max}$	−1679	−1532
	$M_{\text{int.}}^{+\max}$	998	998
	$\lvert M^{-\max}/M_{\text{ext.}}^{+\max}\rvert$	0.62	1.40

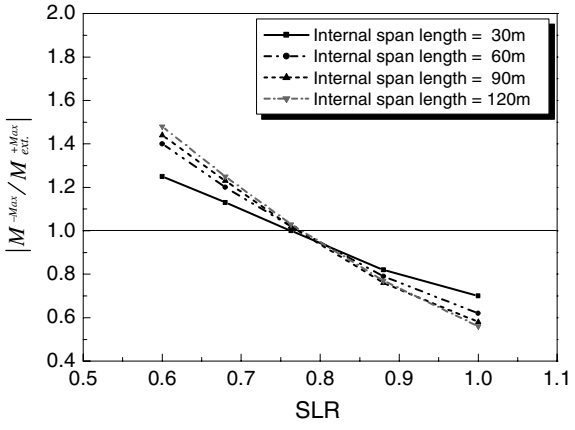

Fig. 17. Relation between $|M^{-\max}/M_{\text{ext.}}^{+\max}|$ and SLR obtained by rigorous analyses.

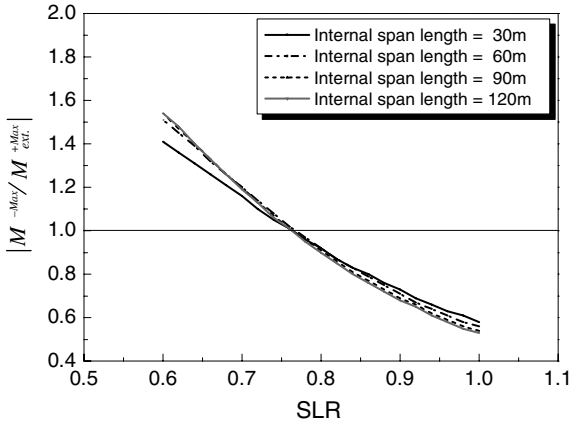

Fig. 18. Relation between $|M^{-\max}/M_{\text{ext.}}^{+\max}|$ and SLR obtained by Eqs. (7)–(9).

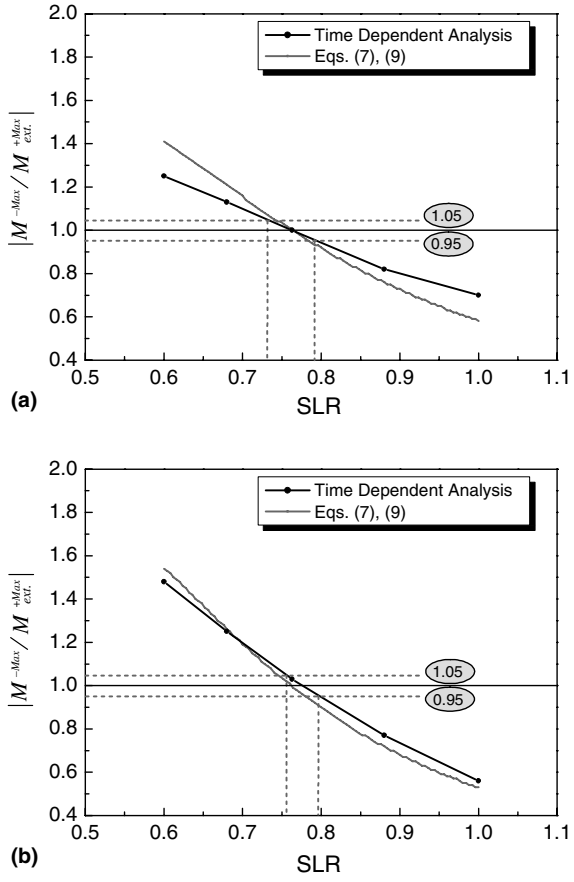

Fig. 19. Relation between $|M^{-\max}/M_{\text{ext.}}^{+\max}|$ and SLR by both methods: (a) $(2L_1 + 0.3)m = 30m$; (b) $(2L_1 + 0.3)m = 60m$.

internal span lengths. Fig. 19 shows the representative comparison of results by both approaches for the internal span lengths of $(2L_1 + 0.3)m = 30m$ and $60m$. As this figure shows, the span length ratio SLR for a rational design of FCM bridges ranges from 0.75 to 0.8 regardless of the internal span length. Finally, the introduced equations can be effectively used in determining an initial section at the preliminary design stage.

In Figs. 20 and 21, the internal moment variations, obtained through rigorous time-dependent analyses, are compared with those obtained by the superposition of both Eqs. (5) and (6) introduced in the companion paper. These figures show that two simple equations introduced in the companion paper effectively simulate the moment distributions regardless of the interior span length. If Eqs. (7)–(9) in this paper, which consider the

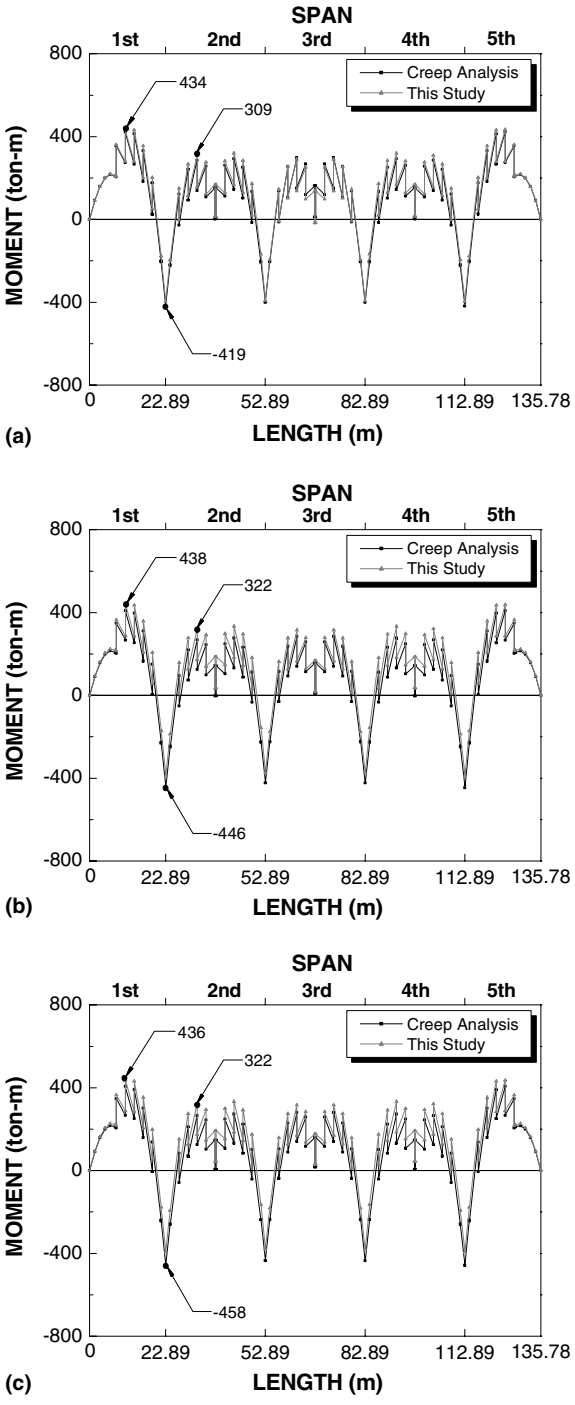

Fig. 20. Moments distribution of $(2L_1 + 0.3)m = 30m$: (a) after 1 year; (b) after 10 years; (c) after 100 years.

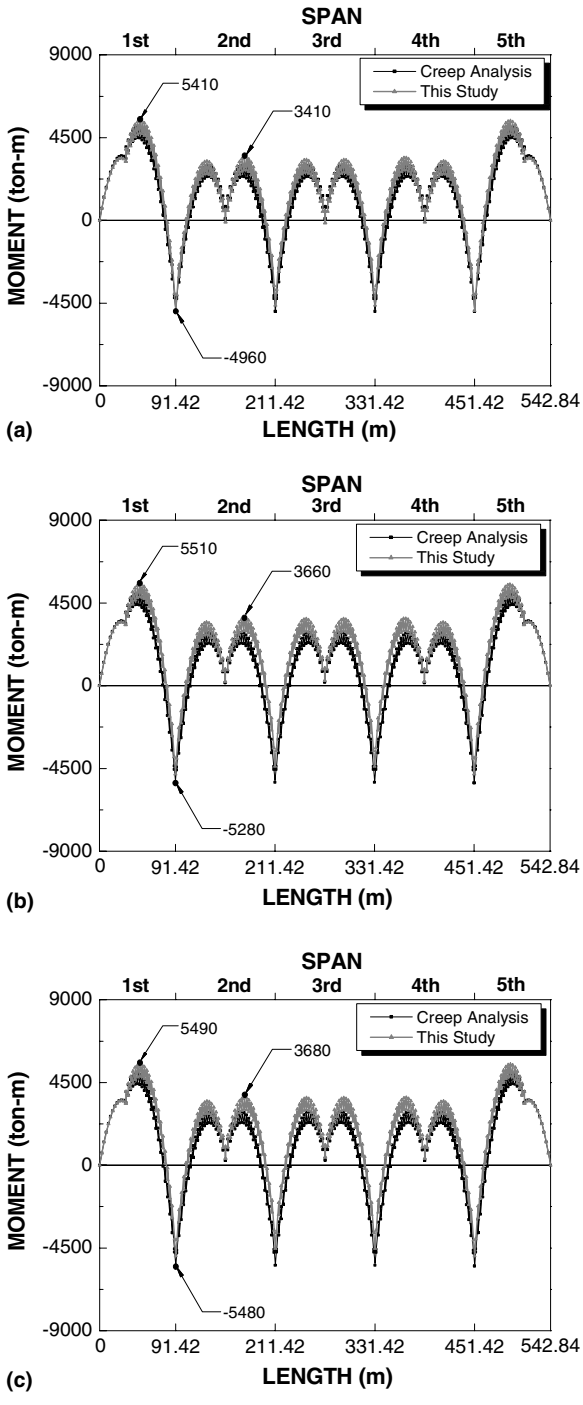

Fig. 21. Moments distribution of $(2L_1 + 0.3)m = 60m$: (a) after 1 year; (b) after 10 years; (c) after 100 years.

relaxation of the cantilever tendons are used together with Eqs. (5) and (6) in the companion paper, then determination of initial trial section dimensions and span length ratio for more rational and effective preliminary design of balanced cantilever bridges may be achieved without a lot of repeated trial processes with rigorous time-dependent analyses.

5. Conclusions

Since concrete bridges constructed by the balanced cantilever method (FCM) experience moment variations due to the change in the structural system during construction, determination of the design moments requires a rigorous time-dependent analysis that considers the

construction sequence. Most numerical analyses, however, have some limitations in wide use because of complexities in practical applications. The design procedure also requires repeated analyses using the initial section changed until a rational design is reached. All of these difficulties combined make a rational and effective design almost impossible. For this reason, simple, but effective, relations to determine the internal moment distributions along all of the spans by the dead load and by the cantilever tendon force are introduced. A relation to determine the span ratio between exterior and interior spans is also introduced.

If an initial cross section and the span length ratio are assumed in the preliminary design stage using the introduced relations, and if a rigorous time-dependent analysis is conducted in the final design stage, then a more improved and effective design may be expected in the case of balanced cantilever bridges. Moreover, a final design can easily be reached without any repeated calculation using a rigorous time-dependent analysis program.

Acknowledgements

The research reported in this paper was made possible by the financial support from the Smart Infra-Structure Technology Center founded by the Korea Science and Engineering Foundation. The authors would like to express their gratitude to this organization for the financial support.

References

[1] Bishara AG, Papakonstantinou NG. Analysis of cast-in-place concrete segmental cantilever bridges. J Struct Eng ASCE 1990;116(5):1247–68.

[2] Chiu HI, Chern JC, Chang KC. Long-term deflection control in cantilever prestressed concrete bridges. I: control method. J Eng Mech 1996;12(6):489–94.

[3] Clemente P, Nicolosi G, Raithel A. Preliminary design of very long-span suspension bridges. Eng Struct 2000;22:1699–706.

[4] Heinz P. RM-spaceframe static analysis of SPACEFRAME. TDA-technische Datenverarbeitung Ges.m.b.H.; 1997.

[5] Hernandez HD, Gamble WL. Time-dependent prestress losses in pretensioned concrete construction. Structural Research Series no. 417, Civil Engineering Studies, Urban: University of Illinois; 1975.

[6] Kang YJ. Nonlinear geometric, material and time dependent analysis of reinforced and prestressed concrete frame. Report no. UC-SEEM 77-1, Berkeley: University of California; 1997.

[7] Kasti FA. Nonlinear material and time dependent analysis of segmentally erected reinforced and prestressed concrete composite 3D frame structures. Report no. UCB/SEMM 90-03, Berkeley: University of California; 1990.

[8] Kwak HG, Seo YJ. Numerical analysis of time-dependent behavior of pre-cast prestressed concrete girder bridges. Construct Building Mater 2002;16:49–63.

[9] Kwak HG, Seo YJ, Jung CM. Effects of the slab casting sequences and the drying shrinkage of concrete slabs on the short-term and long-term behavior of composite steel box girder bridges. Part I. Eng Struct 2000;23:1453–66.

[10] Kwak HG, Seo YJ, Jung CM. Effects of the slab casting sequences and the drying shrinkage of concrete slabs on the short-term and long-term behavior of composite steel box girder bridges. Part II. Eng Struct 2000;23:1467–80.

[11] Kwak HG, Seo YJ. Long-term behavior of composite girder bridges. Comput Struct 2000:583–99.

[12] Lin KY, Frangopol DM. Reliability-based optimum design of reinforced concrete girders. Struct Safety 1996;12(2–3):239–58.

[13] Magura DD, Sozen MA, Siess CP. A study of stress relaxation in prestressing Reinforcement. J PCI 1964;9(2):13–57.

[14] Rath PP, Ahlawat AS, Ramaswamg A. Shape optimization of RC flexible members. J Struct Eng 1999;125(2):1439–46.

[15] Rosignoli M. Nose-deck interaction in launched prestressed concrete bridges. J Bridge Eng 1998;3(1):21–7.